Atomic and electronic structures of niobium clusters

Vijay Kumar[1,2] and Yoshiyuki Kawazoe[1]
[1]*Institute for Materials Research, Tohoku University, 2-1-1 Katahira Aoba-ku, Sendai 980-8577, Japan*
[2]*Dr. Vijay Kumar Foundation, 45 Bazaar Street, Chennai 600 078, India*
(Received 16 July 2001; revised manuscript received 19 November 2001; published 20 February 2002)

First-principles electronic structure calculations have been carried out on Nb_N clusters with $N=2-23$ atoms using ultrasoft pseudopotentials, a plane wave basis and generalized gradient approximation for the exchange-correlation energy, to elucidate the growth behavior and the evolution of the electronic structure. Our results show that clusters with $N>13$, prefer high coordination structures with hexagonal antiprisms except for $N=15$ which has a distorted body centered cubic structure (bcc). Clusters with $N>2$ favor lowest spin configurations. Of particular importance is the finding that icosahedral growth is not favored in these clusters. There are large highest occupied-lowest unoccupied molecular orbital (HOMO-LUMO) gaps for clusters with 4, 6, 8, 10, and 16 atoms. These are in agreement with the observed low reactivities as well as the photoemission data of 6-, 8-, 10-, and 16-atom clusters. Clusters with 4, 8, 10, 15, and 16 atoms are found to be magic, suggesting the importance of the atomically closed shell bcc structure of Nb_{15} even though the HOMO-LUMO gap is small. However, Nb_6 is not magic. A dimerization behavior is obtained in Nb_{10} and it is found to be even more prominent in the isoelectronic V_{10}. But, this tendency is absent in Ta_{10}. The calculated binding energies, electronic structures and fragmentation behavior are in good agreement with available experimental data.

DOI: 10.1103/PhysRevB.65.125403 PACS number(s): 36.40.Cg, 73.22.−f

I. INTRODUCTION

Atomic and electronic structures of transition metal clusters play an important role in understanding their growth behavior, and associated catalytic, magnetic, thermal and optical properties. Several experimental studies[1] on abundance, ionization potential (IP), photoemission, reactivity and magnetic behavior show size specific properties of transition metal clusters. However, theoretical studies of such clusters have been difficult due to the presence of *d* electrons that also lead to their different magnetic behavior from bulk. This is important from the point of view of nanodevices. A relatively simple but interesting case is the growth behavior of niobium clusters. Niobium is nonmagnetic in bulk but small clusters could have magnetic moments due to the odd number of valence electrons in Nb atom. This could also lead to significant even-odd alternation in cluster properties. Reactivities of niobium clusters with hydrogen show dramatic size dependence[2–4] that is quite different from the behavior known for clusters of some other transition metals such as nickel.[5] In particular low reactivities of hydrogen and nitrogen[4] have been obtained for niobium clusters with 8, 10, and 16 atoms. Similar studies[6] of CO reactivity with neutral Ni and Nb clusters show different behaviors with a distinct minimum for Nb_{10}. However, niobium as well as nickel clusters with more than 20 atoms do not show significant size dependent reactivities. This suggests that the electronic structures of small clusters of these two elements are different and that there are effects specific to niobium that make some of its clusters behave quite distinctly from normally reactive behavior of transition metals. Photoemission studies[2] on niobium clusters suggest large HOMO-LUMO gaps for 8-, 10-, and 16-atom clusters. Also the IPs of these magic clusters are high[7] and these could be responsible for their low reactivities. In general, from the point of view of the electronic structure, a partially occupied $4d$ band in niobium should make its clusters quite reactive as also the surfaces of bulk niobium. This is indeed reflected in the behavior of large clusters. Therefore, the different behavior of small clusters is interesting for developing a proper understanding of the phenomena occuring in transition metal clusters.

The abundance spectrum of niobium clusters shows magic behavior that is different from the often observed[1] icosahedral growth in metal clusters[1] such as Sr, Ba, and Ni, with $N=7,13,19,\ldots$. It suggests an important role of the electronic structure in the growth behavior of these clusters. Large HOMO-LUMO gaps and high IPs due to electronic shell closing are typical for magic clusters of sp bonded metals.[1] However, for niobium, the main contribution to bonding comes from the $4d$ electrons and as such the jellium picture is inappropriate for such materials. In bulk the stability of the bcc structure of niobium is related[8] to the existence of a pseudogap in the middle of the band such that predominantly the e_g states are occupied while the t_{2g} states are empty. In clusters, the band narrows due to a lower mean coordination as compared to the bulk. It could lead to a significant gap for certain clusters of such bcc elements.

The vertical detachment energies[2] of Nb_6-Nb_{17} clusters show an even/odd alternation similar to the behavior found in simple metal clusters. This suggests that clusters with even number of atoms have closed electronic shell structures. However, in a different experiment,[9] mass spectrum of autoionized niobium clusters showed marked intensities for $N=7$, 13, 15, and 22 with magic behavior for 7, 15, and 22 and a minimum in the abundance intensity for $N=19$. Another recent study[10] also showed magic behavior for 7- and 15-atom cation clusters. Therefore, the reactivities and the stabilities of these clusters have different behaviors. It is possible that the reactivity of the neutral 7 and 15 atom clusters is due to the odd number of electrons that, as we shall show later, also leads to their small HOMO-LUMO gaps. On the

other hand, the particular stability may be associated with the atomically close shell structures of such clusters.

An important property of transition metal clusters is the occurrence of magnetism. The odd number of valence electrons in niobium atom as well as the band narrowing could give rise to magnetism in small clusters. Photoemission data[2] suggest that these clusters exist in the lowest spin state except for Nb_3 and Nb_5. An important question in the growth of clusters is the smallest size for which clusters attain bulklike behavior. Photoemission studies[2] show the spectrum of Nb_{15}^- to have features that are different from those obtained for other clusters. It has been suggested that this could be due to the bcc closed atomic shell structure of this cluster as in the bulk. But so far there has been no theoretical study on niobium clusters with more than 10 atoms. The reactivities of cation and anion niobium clusters[11,12] have been found to be similar. This has been considered to be an indication for the importance of the geometric effects. The electronic and atomic structures are, however, correlated and therefore, it is of interest to understand these and their correlation with reactivities.

Theoretical studies on the growth behavior and electronic structure of niobium clusters have been carried out in the small size range with up to 10 atoms. Goodwin and Salahub[13] studied clusters having up to 7 atoms using spin-polarized local and nonlocal density functional theories. The growth was found to be close packed. Kietzmann *et al.*[14] and Fournier *et al.*[15] have performed local spin density (LSD) functional calculations with a model core potential to describe the inner shells and the valence electrons of anion clusters with $N=3-8$. Their results of the atomic structures are similar to those of neutral clusters. From studies on isomers of 8- to 10-atom clusters they obtained large HOMO-LUMO gaps for Nb_8 and Nb_{10} as also found in the photoemission experiments.[2] Grönbeck and Rosén[16] have studied clusters with $N\leqslant 10$ in the LSD approximation and found high coordinated structures to have lower energies. Structural, electronic and vibrational properties of neutral and charged 8- to 10-atom clusters have been studied by Grönbeck *et al.*[17] within LSD as well as gradient corrected exchange correlation density functional of Becke,[18] Lee, Yang, and Parr[19] (BLYP). Generally the lowest energy structures of the neutral and charged clusters were found to be similar.

Here we present results of the atomic and electronic structures of neutral niobium clusters having up to 23 atoms and discuss the growth and evolution of the electronic structures in the light of the experimental results. The exceptional stability of 10-atom clusters has been further explored for isoelectronic V_{10} and Ta_{10} clusters in order to find the commonality of the electronic structure and the magic behavior.

II. COMPUTATIONAL METHOD

The calculations have been performed using *ab initio* ultrasoft pseudopotential method.[20,21] A plane wave expansion is used with a cutoff of 12.84 Ry for the wavefunctions. The exchange-correlation energy is calculated within the generalized gradient approximation.[22] For all clusters with odd number of valence electrons we performed spin-polarized calculations. In most cases of even atom clusters, spin-unpolarized calculations were done. However, for dimer and in the cases of isomers of even atom clusters with high symmetric structures, spin-polarized calculations were also performed. However, these were found to lie higher in energy except for the dimer. A simple cubic supercell of size up to 18.0 Å is used with periodic boundary conditions. For such large cells the Γ point is sufficient for Brillouin zone integrations. It was found necessary to include the $4p$ states also as valence because with only outer 5 valence electrons some of the bond lengths were obtained to be unphysically short in initial calculations on several clusters. All the results presented in the following section are obtained considering 11 valence electrons in Nb atom. We optimized several isomers of a cluster using conjugate gradient technique to explore the lowest energy isomers.

The ground state of Nb_2 is found to have a magnetic moment of $2\ \mu_B$ with a bond length of 2.15 Å. This is a very short bond as compared to the experimental bulk value of 2.85 Å and the calculated GGA bulk value of 2.869 Å. It reflects strong bonding due to $4d$ electrons. The binding energy (BE) is 4.43 eV. This is an underestimate as compared to the experimental value[23] of 5.24 ± 0.13 eV and 4.86 ± 0.02 eV.[24] The LSDA values[16] are 5.68 eV and 2.11 Å whereas the nonlocal values[13] are 5.4 eV and 2.10 Å for the BE and bond length, respectively. However, as we shall show, the agreement with the experimental values of the BE becomes better for larger clusters. In general, we find that the calculated bulk BE of 6.893 eV/atom is also an underestimation as compared to the experimental value of 7.57 eV/atom. Therefore, GGA overcorrects the overbinding of LDA, though the bond lengths are in excellent agreement with experiments.

III. RESULTS

The results of the structures of different isomers studied here, as well as the BEs and HOMO-LUMO gaps are given in Tables I and II. The nearest neighbor bond lengths were truncated at 3.25 Å. In the following we discuss these results in detail.

A. Structures and growth behavior

Nb_3-Nb_{11}. Nb_3 is an isosceles triangle with sides 2.29, 2.42, and 2.42 Å and spin multiplicity 2. These are in good agreement with the values of 2.26, 2.37, and 2.37 Å obtained by Goodwin and Salahub[13] and 2.25, 2.40, and 2.40 Å by Gronbeck and Rosen[16] using LSDA. The BE is 3.03 eV/atom which agrees well with the experimental value[23] of 3.27 ± 0.11 eV/atom. Figure 1 shows different isomers of Nb_4 to Nb_{11} clusters obtained from the present study. Nb_4 is a regular tetrahedron with side 2.53 Å and zero spin. This is the only cluster with perfect symmetry. This is in agreement with the results obtained in Ref. 13, where the bond length was reported to be 2.47 Å but it differs from a slightly distorted tetrahedron with sides 2.51 and 2.52 Å obtained in Ref. 16. The calculated BE is 3.74

TABLE I. Structure, BE (eV/atom), HOMO-LUMO gap (eV), and the nearest neighbor bond lengths (Å) for Nb_N clusters. PBP and HBP refer to pentagonal and hexagonal bipyramids, respectively. Generally, even (odd) atom clusters have 0 (1) μ_B magnetic moment. In cases, where these are different, values have been given in brackets.

N	structure	BE	Gap	*d*
2	dimer ($2\mu_B$)	2.22	0.48	2.15
3	isosceles triangle	3.03	0.49	2.29,2.42
4	tetrahedron	3.74	1.20	2.53
5	capped rhombus	3.96	0.32	2.48–2.83
6a	Distorted prism	4.18	0.43	2.42–2.94
6b	tetrahedral	4.15	0.10	2.44–2.95
6c	octahedral	4.05	0.31	2.46–3.14
7	PBP	4.46	0.20	2.47–2.91
8a	Bicapped octahedron	4.65	0.78	2.52–3.25
8b	Bicapped prism	4.57	0.80	2.52–3.24
9a	Tricapped prism	4.68	0.30	2.48–2.94
9b	capped PBP	4.66	0.22	2.42–2.89
10a	Bicapped antiprism	4.85	0.99	2.43–2.86
10b	hexagonal	4.74	0.54	2.49–3.00
10c	another hexagonal type	4.66	0.58	2.45–3.12
11a	2 fused PBP	4.77	0.25	2.48–3.12
11b	Capped HBP	4.76	0.30	2.48–3.12
11c	capped trigonal prism	4.63	0.12	2.51–3.05
11d	cubic	4.43	0.15	2.56–3.19

eV/atom which is also in close agreement with the experimental value of 3.90 ± 0.16 eV/atom. The pentamer is a distorted trigonal bipyramid with a spin multiplicity 2. It has an isosceles triangle base with sides 2.67 and 2.83 Å. The base to pole distances are 2.48 and 2.60 Å. This is in contrast to the finding of a symmetric trigonal bipyramid in Refs. 13 and 16. In fact this cluster could be best described as a capping of a bent rhombus of side 2.48 Å. The BE is 3.96 eV/atom as compared to the experimental value of 4.21 ± 0.19 eV/atom. For Nb_6, we optimized an octahedron, a prism and a tetrahedral structure. The lowest energy structure is found to be a distorted prism (6a in Fig. 1) with zero spin. The base is a parallelogram and there are some short bonds (2.42 Å). The overall bond lengths vary in the range of 2.42-2.94 Å. A tetrahedral structure (6b) as reported in Refs. 13 and 16, lies 0.2 eV higher in energy, while a relaxed octahedron (6c), 0.79 eV higher in energy. The calculated BE (4.18 eV/atom) is in good agreement with the experimental value of 4.44 ± 0.20 eV/atom. We find the lowest energy isomer to have a larger gap (0.43 eV) as compared to other isomers and this is important for understanding the lower reactivity of Nb_6.

Nb_7 is a distorted pentagonal bipyramid as also obtained earlier in Refs. 13 and 16. The calculated equitorial bond lengths are 2.53, 2.54, 2.60, and 2.65 Å whereas the polar-

TABLE II. Same as in Table I.

N	structure	BE	Gap	*d*
12a	Capped HBP	4.84	0.39	2.45–3.10
12b	bicapped Nb_{10}	4.76	0.61	2.37–3.12
12c	hexagonal ($2\mu_B$)	4.73	0.10	2.45–2.95
12d	Capped fused prism	4.71	0.35	2.46–3.04
13a	relaxed icosahedron	4.88	0.19	2.39–3.12
13b	relaxed cuboctahedron ($3\mu_B$)	4.84	0.08	2.55–3.05
13c	fused HBP-PBP	4.78	0.23	2.38–3.19
14a	Capped hexagonal antiprism	5.02	0.33	2.40–3.13
14b	cubic ($2\mu_B$)	4.99	0.13	2.57–3.14
14c	capped Nb_{13}	4.96	0.48	2.48–3.12
15a	Cubic	5.14	0.15	2.62–3.10
15b	Capped hexagonal antiprism	5.11	0.194	2.47–3.10
16a	hexagonal	5.16	0.47	2.36–3.02
16b	cubic (face capping)	5.06	0.10	2.42–3.17
16c	hexagonal (face capping)	5.05	0.12	2.39–3.10
16d	hexagonal (side capping)	5.05	0.19	2.47–3.10
16e	cubic (edge capping)	5.04	0.61	2.25–3.18
17a	Hexagonal	5.14	0.18	2.50–3.23
17b	cubic	5.08	0.16	2.40–3.25
18a	hexagonal	5.14	0.22	2.39–3.06
18b	hexagonal	5.09	0.24	2.41–3.24
18c	icosahedral	5.00	0.25	2.48–3.24
19a	hexagonal	5.14	0.08	2.49–3.14
19b	icosahedral	5.07	0.14	2.45–3.24
20a	hexagonal	5.18	0.25	2.46–3.25
20b	hexagonal	5.13	0.36	2.54–3.11
20c	icosahedral	5.13	0.29	2.48–3.23
20d	cubic	5.03	0.16	2.54–3.25
21	hexagonal	5.22	0.17	2.55–3.16
22a	hexagonal	5.27	0.17	2.47–3.08
22b	hexagonal	5.26	0.21	2.46–3.14
23a	hexagonal	5.31	0.12	2.47–3.13
23b	icosahedral	5.15	0.06	2.46–3.33
23c	decahedral ($3\mu_B$)	5.02	0.14	2.36–3.25

equitorial bond lengths are 2.47, 2.56, 2.60, 2.77, 2.81, 2.85, and 2.90 Å. The pole to pole bond length is 3.23 Å. The BE is 4.46 eV/atom as compared to the experimental value of 4.74 ± 0.21 eV/atom. For Nb_8, we tried several structures such as D_{2d}, capped prism and a capped octahedron. The lowest energy structure is a bicapped distorted octahedron (8a in Fig. 1). This has a large basin of attraction and more than one structure transforms to this isomer on relaxation. From the point of view of growth, it is interesting that this structure can be viewed as the one obtained from capping of a pentagonal bipyramid, or from bicapping of the Nb_6 structure. It is rich in rhombuslike (flat and bent) local arrange-

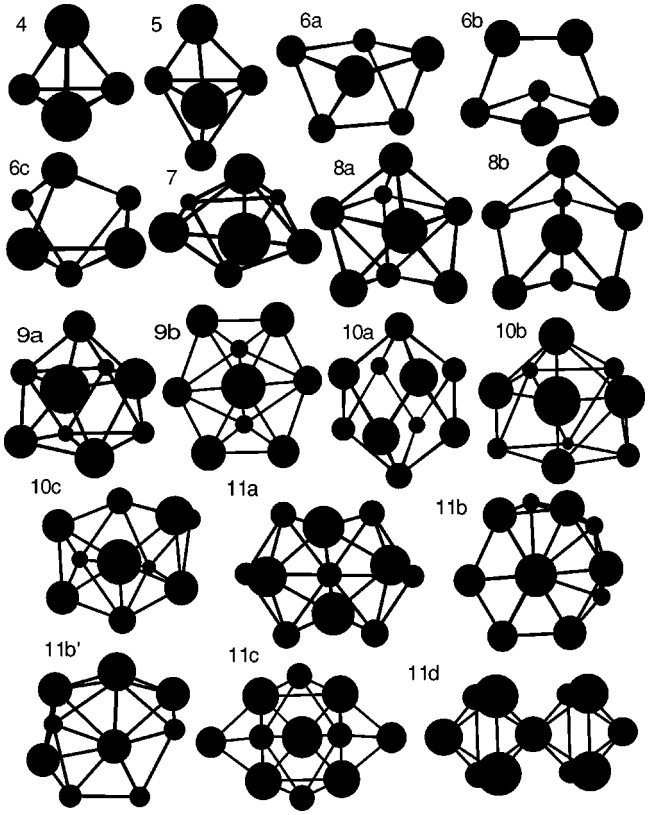

FIG. 1. Projections of atomic structures of low lying isomers of Nb_N ($N=4-11$) clusters. The smaller the size of the atom, the farther it is down the page.

ments which are also seen in smaller clusters. The bond lengths vary in the range of 2.52–3.25 Å. A similar structure was obtained for the anion cluster by Kietzmann *et al.*[14] and for neutral cluster by Grönbeck *et al.*[17] However, this result differs from a capped hexagonal ring structure obtained in Ref. 16. The BE is 4.65 eV/atom and it agrees well with the experimental value of 4.90 ± 0.24 eV/atom. Another structure with a bicapped prism geometry (8b) lies 0.61 eV higher in energy. There is some similarity in the two relaxed structures and indeed Nb_9 is found to be a distorted tricapped prism (9a). Another view of this structure is a triangle capping a distorted pentagonal pyramid or a near rhombus capping a rectangle. The latter is interesting as the bonds within rectangle are 2.71 and 2.94 Å and in the rhombus, 2.57 and 2.59 Å. But some of the inter-rectangle-rhombus bonds are shorter with values 2.48 and 2.52 Å while others have values 2.70 and 2.91 Å. The existence of short bonds shows a tendency for dimerization as we shall show for Nb_{10}. This isomer is different from a hexagon with cappings of one and two atoms on the two faces (9b) obtained in Refs. 16 and 17 within LSDA (another view of this structure is two fused pentagonal bipyramids). This lies 0.13 eV higher in energy. However, Gronbeck *et al.*[17] obtained a tricapped prism to be of lowest energy using BLYP, in agreement with our results. For Nb_{10} several structures were considered including, a bicapped antiprism, a T_d structure and a capped prism. The lowest energy structure is a bicapped antiprism (10a in Fig. 1). This could also be considered to arise from capping of a prism. It has high rotational symmetry with all the bonds from the two capping atoms to the antiprism being equal to 2.56 Å while the bonds between the two nearly square faces alternate with values of 2.43 and 2.73 Å. Therefore, there is a dimerization in this cluster. The bond lengths within the faces themselves are longer with the value of 2.86 Å. The BEs for Nb_9 and Nb_{10} are 4.68 and 4.85 eV/atom in good agreement with the experimental values of 4.93 ± 0.25 and 5.09 ± 0.27 eV/atom, respectively. The BE of Nb_{10} has a local maximum which could be the reason for its strong magic behavior. Two other isomers based on capping of a pentagonal pyramid by a near rhombus (10b) and two fused pentagonal bipyramids (10c) which can be obtained from capping of (9b) lie 1.178 and 1.956 eV higher in energy, respectively. These results suggest significantly lower energy of the (10a) isomer which could lead to a strong abundance of this isomer in experiments.

The two lowest energy isomers of Nb_{11} are shown in Fig. 1 (11a and 11b). The one with the lowest energy (11a) can be described as two pentagonal bipyramids fused at a triangular face. The bond lengths vary significantly and lie in the range of 2.48–3.12 Å. This behavior is in fact common to most of the clusters. The other isomer can be described as a capped hexagonal bipyramid (11b) or a capped pentagonal bipyramid (11b′ is another view of 11b). The bond lengths in this case also vary in the range of 2.48–3.12 Å. Both these isomers are nearly degenerate with BE's 4.77 and 4.76 eV/atom, respectively. This agrees well with the experimental value of 5.12 ± 0.28 eV/atom. We also calculated a pentacapped prism (11c) and a bicapped (opposite faces) body centered cube (11d). The two lie 1.56 and 3.78 eV higher in energy than the isomer 11a. Also the cube has a magnetic moment of $3\mu_B$.

Nb_{12}-Nb_{23}. The low lying isomers of 12- to 23-atom clusters are shown in Figs. 2–4. The lowest energy structure of Nb_{12} can be described as capping of a distorted hexagonal bipyramid or a capped pentagonal bipyramid (12a). The bond lengths vary from 2.45 to 3.10 Å. Another structure (12b) based on a dimer capping of (10a) lies 0.92 eV higher in energy. This is a relatively large difference in energy and it is significant in the light of the strong magic behavior of Nb_{10}. Furthermore, this isomer has a significant HOMO-LUMO gap (0.61 eV). It is to be noted that in some experiments[12] Nb_{12} has also been found to be less reactive. We further considered a hexagon with three atoms capping on either side. The optimized structure relaxes significantly and is shown in (12c). It lies 1.30 eV higher in energy than the isomer (12a) and has a magnetic moment of $2\mu_B$. Another structure (12d) based on two fused prisms with capping of 4 atoms (a different view of this is a distorted capped cube) lies 1.51 eV higher in energy than (12a).

13-atom clusters of many transition metals are found[1] to have an icosahedral structure. However, for Nb_{13} it is not even a local minimum. It relaxes to a structure (13a) shown in Fig. 2. It has threefold rotational symmetry as it can be seen in (13a) with elongated bonds between three atoms. The bond lengths vary significantly and lie in the range of 2.39–3.12 Å. The BE is 4.88 eV/atom. In an icosahedron the center to vertex bond length is about 5% shorter than the

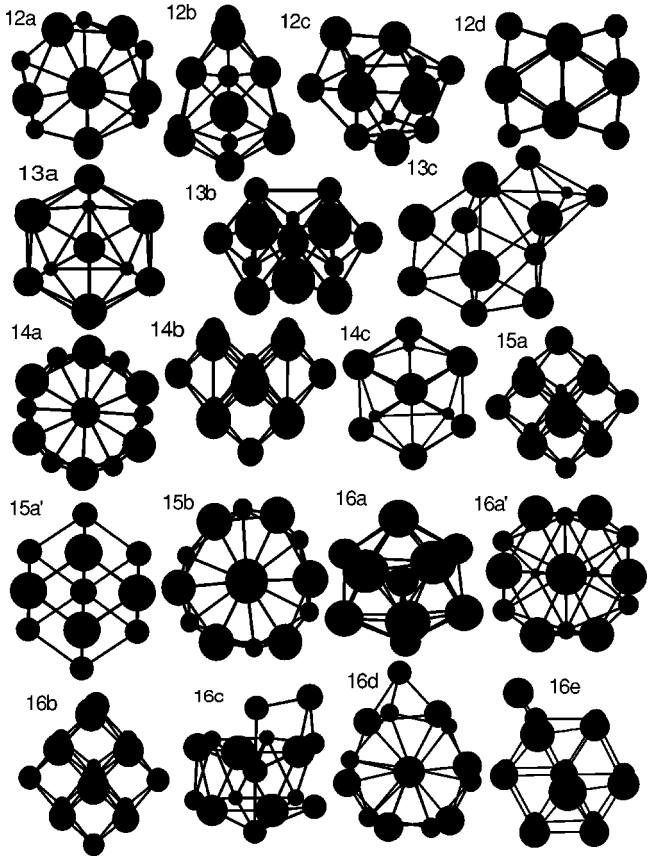

FIG. 2. Same as in Fig. 1 but for $N=12-16$.

nearest vertex to vertex bond length. Therefore the surface atoms in an icosahedron are not optimally bonded. This leads to an inward pressure on the core of an icosahedral cluster. Studies[25] on strontium clusters showed that elements with large compressibilities are more likely to exhibit icosahedral growth of their clusters. In the middle of a *d* series, compressibility reduces, making icosahedral growth difficult. Another isomer (13b), obtained from relaxation of a cuboctahedral structure converges to a high spin state with $3\mu_B$ magnetic moment. It lies 0.53 eV higher in energy. The nearest neighbor bond lengths in this isomer are slightly elongated as compared to isomers 13a and 13c that have a lower spin magnetic moment. An isomer with fused hexagonal bipyramid-pentagonal bipyramid (13c) structure lies 1.268 eV higher in energy than the isomer (13a) and has BE of 4.78 eV/atom.

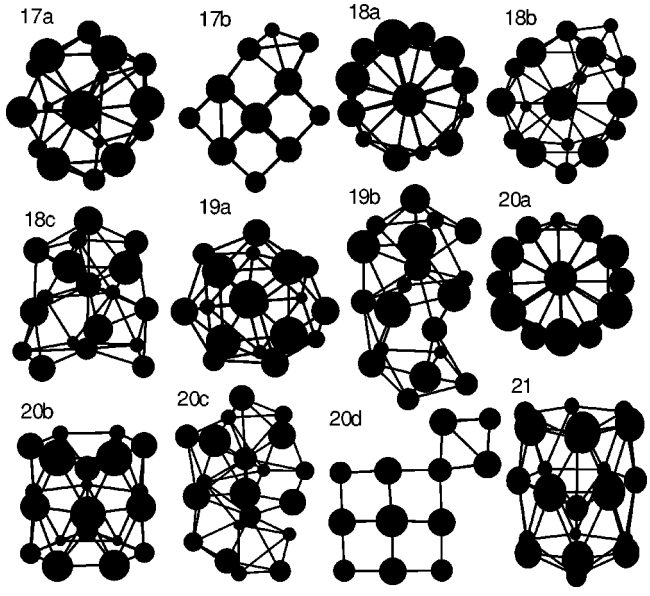

FIG. 3. Same as in Fig. 1 but for $N=17-21$.

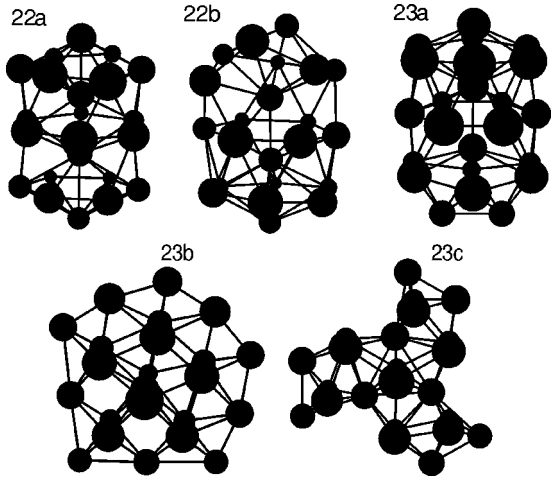

FIG. 4. Same as in Fig. 1 but for $N=22$ and 23.

For Nb_{14}, we tried a capped icosahedron, a hexagonal layered structure, symmetric capping of the lowest energy Nb_{13}, and a bcc structure. Capped icosahedron relaxes significantly and lies highest in energy. This result together with the instability of an icosahedron for Nb_{13} suggests that *niobium clusters do not favor icosahedral growth*. This result confirms the correlation between high compressibility and icosahedral growth suggested by us earlier.[25] Niobium has low compressibility and therefore, it is not surprising that icosahedral growth is not favored. The lowest energy isomer of Nb_{14} is a hexagonal antiprism with an atom at the center and one face capped (14a). The other two (14b and 14c) are nearly degenerate. The BE's of the four isomers are 4.89, 5.02, 4.98, and 4.96 eV/atom, respectively. The bond lengths for the lowest energy isomer have significant spread with values lying in between 2.40 and 3.13 Å. This reduces the rotational symmetry from sixfold to twofold. Also isomer (14c) has significantly higher gap. As this is derived from the lowest energy isomer of Nb_{13}, it is possible that it is present in experimental conditions and could show low reactivity. The cubic isomer (14b) has a magnetic moment of $2\mu_B$. This could be a reason for the slightly elongated bond lengths in this cluster as also observed for isomer 13b.

For Nb_{15}, we optimized two isomers: a bcc structure and a capped hexagonal antiprism structure. bcc structure has been proposed for this cluster as the peaks in the photoemission data are quite different from those of other clusters. We find that this cubic isomer (15a) indeed has the lowest BE (5.14 eV/atom), though cubic structure is not of lowest energy for Nb_{14}. However, the symmetry is not fully cubic. Slight distortions make threefold rotation to be the highest

symmetry and the bond lengths are in the range of 2.62–3.10 Å. As compared to other clusters, this does not have short bonds. (15a′) shows another view of this cluster such that a hexagonal layer with center atom is capped with a rhombus above and below. The hexagonal isomer lies only 0.53 eV higher in energy and is likely to be present in experiments. It has distortions and the bond lengths vary from 2.47 to 3.10 Å.

We studied several isomers of Nb_{16} as it is another cluster which shows magic behavior. The lowest energy isomer is shown in Fig. 2 (16a). It is obtained from Nb_{13} by capping three atoms on the face with three elongated bonds. This can also be viewed as an hexagonal antiprism structure in which on one side of a layer there are two atoms as shown in (16a′). One atom caps the other layer and there is an atom at the center. There are many ways of capping the hexagonal structure and this is found to have the lowest energy. Capping of the Nb_{15} cubic structure leads to an isomer (16b) which lies 1.71 eV higher in energy. Also capping of the 15-atom hexagonal structure with an atom adjacent to a polar atom (16c) leads to an isomer which lies 1.80 eV higher in energy. Capping on a side (16d) leads to an isomer which is 1.88 eV higher in energy. Capping an atom on an edge of the bcc isomer (16e) leads to a structure that is 1.997 eV higher in energy. These results support the particular stability of the Nb_{15} cluster and suggest that the lowest energy structure of Nb_{16} may be uniquely abundant. In this the central atom has 15 neighbors in the range of 2.36–3.02 Å. These are also the shortest and longest nearest neighbor bonds in this cluster. Therefore, niobium clusters favor high coordinated structures. This is presumably due to the fact that the *d* states are less than half-filled and their energy can be lowered by increasing the coordination.

Isomers of Nb_{17} to Nb_{21} clusters are shown in Fig. 3. Continuing the trend of hexagonal structures, Nb_{17} is obtained from Nb_{16} by adding an atom such that instead of a dimer, there is a trimer on one side (17a in Fig. 3). The central atom has 16 nearest neighbors within a range of 2.67–3.23 Å. This is the highest coordinated cluster. In the whole cluster, the bond lengths vary between 2.54 and 3.23 Å. Another isomer based on a cubic structure (17b) lies 1.05 eV higher in energy. This is capping of the Nb_{15} structure by a dimer.

The structure of Nb_{18} is a continuation of the Nb_{16} structure such that instead of two atoms, now four atoms cover one of the hexagonal faces with a rhombus structure (18a in Fig. 3). There are 14 nearest neighbors of the central atom in the range of 2.67–3.01 Å. The bond lengths vary in between 2.39 and 3.06 Å. Another isomer in which three atoms form a triangle and one atom is nearest neighbor to one of these (18b), lies 0.93 eV higher in energy. An isomer based on double icosahedral packing (one vertex atom missing) is distorted (18c) and lies 2.60 eV higher in energy. Therefore, hexagonal isomer continues to be favored.

The lowest energy structure of Nb_{19} is shown in (19a) of Fig. 3. This has intertwined capped pentagons and hexagons and two nearly square faces rotated with respect to each other by about 45°, each one being capped by an atom. The central atom has 16 nearest neighbors, 14 in the range of 2.68 and 3.14 Å and two at a distance of 3.43 Å. The other structure (19b) is based on a double icosahedron which is distorted. Three different minimizations led to slightly differing structures in the way distortion occurred. Their energies are quite similar and lie more than 1.35 eV higher than the value for the (19a) isomer. The 19-atom cluster is also often found to have a double icosahedral structure for several metal clusters. These results, therefore, reaffirm that icosahedral growth is not favored by niobium clusters.

For Nb_{20} we tried several structures based on hexagons, cube and icosahedron. The lowest energy isomer is based on the capping of the hexagonal isomer of Nb_{15} with five atoms on one of the hexagonal faces (20a). The isomer in which two capping atoms are symmetrically missing from the two hexagonal faces (20b) lies 0.91 eV higher in energy. Another isomer based on icosahedral structure but with a hexagon in the middle (20c) lies 0.95 eV higher in energy while a cubic isomer (20d) lies significantly higher in energy (2.96 eV). The bond lengths in the lowest energy isomer are in the range of 2.51–3.26 Å. Nb_{21} is based on a double hexagonal antiprism with one capping atom missing.

Lowest energy structures of Nb_{22} (22a) and Nb_{23} (23a) are also based on a double hexagonal antiprism (Fig. 4). For Nb_{22}, we tried another isomer based on icosahedral structure. It distorts significantly and leads to a structure (22b) that is similar to the hexagonal isomer. For Nb_{23}, we optimized hexagonal isomer with two atoms capping a hexagonal face instead of one as in Nb_{22}, a decahedral and an icosahedral structure. Again, hexagon based isomer has the lowest energy. The other two lie significantly higher in energy (Table II). A decahedral isomer distorts significantly (23b) and an icosahedral isomer opens up (23c) as in Nb_{13}.

These results suggest that clusters with hexagonal isomers become favorable in the size range of $N>13$ except for $N=15$ for which a bulk fcc type structure has the lowest energy. In the smaller size range the growth behavior shows competition between the tetrahedral and prism based growths. In almost all cases there are some short bonds and in the case of Nb_{10}, dimerization is particularly evident. It should be pointed out here that for chromium clusters,[26] the structures are based on dimers with very short bonds. So it appears that in the middle of a *d* series, there is a tendency for dimerization in clusters to increase the *d*-*d* bonding. In niobium clusters this tendency is weaker and it gets further weakened with an increase in the cluster size such that there is a preference for structures with higher coordination.

B. Electronic structure

The electronic spectra of the lowest energy isomers of all the clusters are shown in Figs. 5–8 with a Gaussian broadening of the levels. For the dimer and clusters with odd number of atoms, we have also shown the spin decomposed density of states (DOS). It is seen from Fig. 5 that for Nb_2 the exchange splitting is large (0.5 eV) but it decreases significantly with an increase in the cluster size such that all clusters favor the lowest spin states except for the dimer. The occupied density of states of small clusters having up to 10 atoms can be grossly described to have prominent features

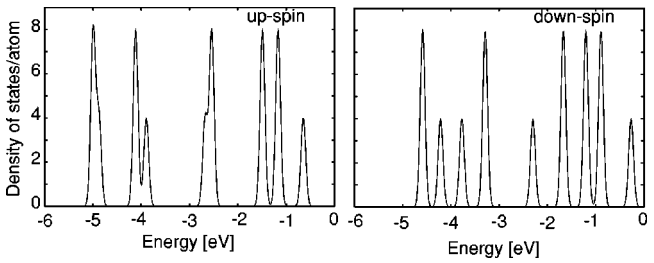

FIG. 5. Gaussian (width 0.1 eV) broadened electronic spectra of up- and down-spin components of Nb_2. The exchange splitting of states can be easily noticed.

around -3.5, and -4.0–5.0 eV, all associated mainly with $4d$ electrons. The photoemission spectra[2] have been obtained for anion clusters and in most cases there are sharper peaks for clusters with odd number of atoms (even number of electrons) as compared to clusters with even number of atoms (odd number of electrons). On the other hand, neutral clusters with even number of atoms are likely to have sharper features due to spin degeneracies. Furthermore, the photoemission peaks for anion clusters are likely to be shifted to lower binding energies as compared to the density of states of the neutral clusters. There could also be some thermal broadening of the spectra. In the following we, therefore, compare only the gross features.

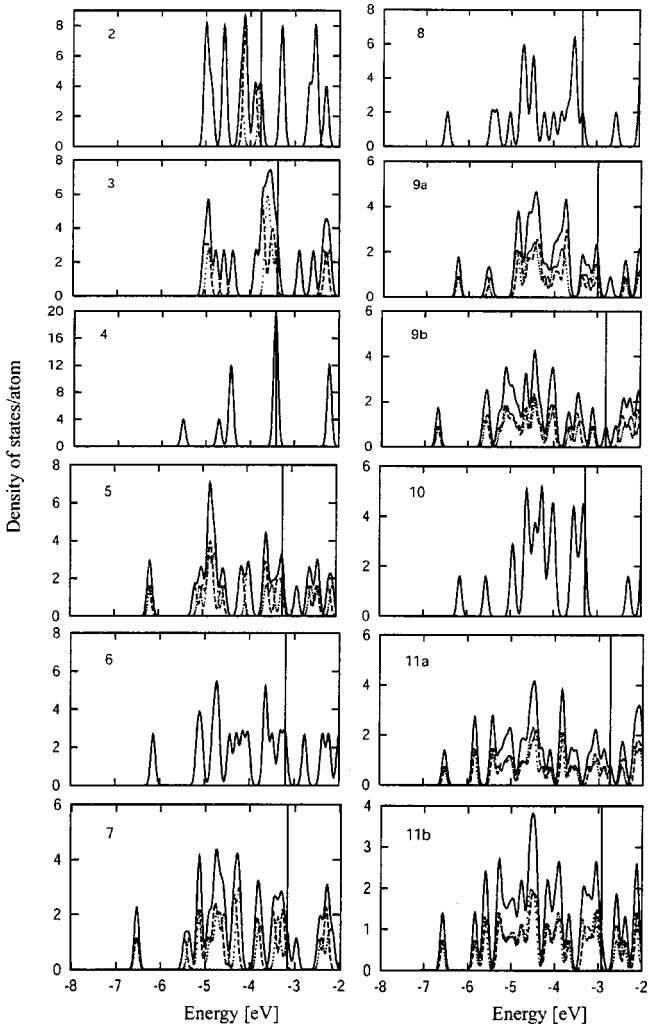

FIG. 6. Gaussian broadened total electronic states of the lowest energy isomers of Nb_N clusters. 9b and 11b are nearly degenerate with 9a and 11a, respectively. For $N=2$ and odd values, the spin-up (broken line) and spin-down (dots) components of the spectra are also shown. Vertical line shows the Fermi level.

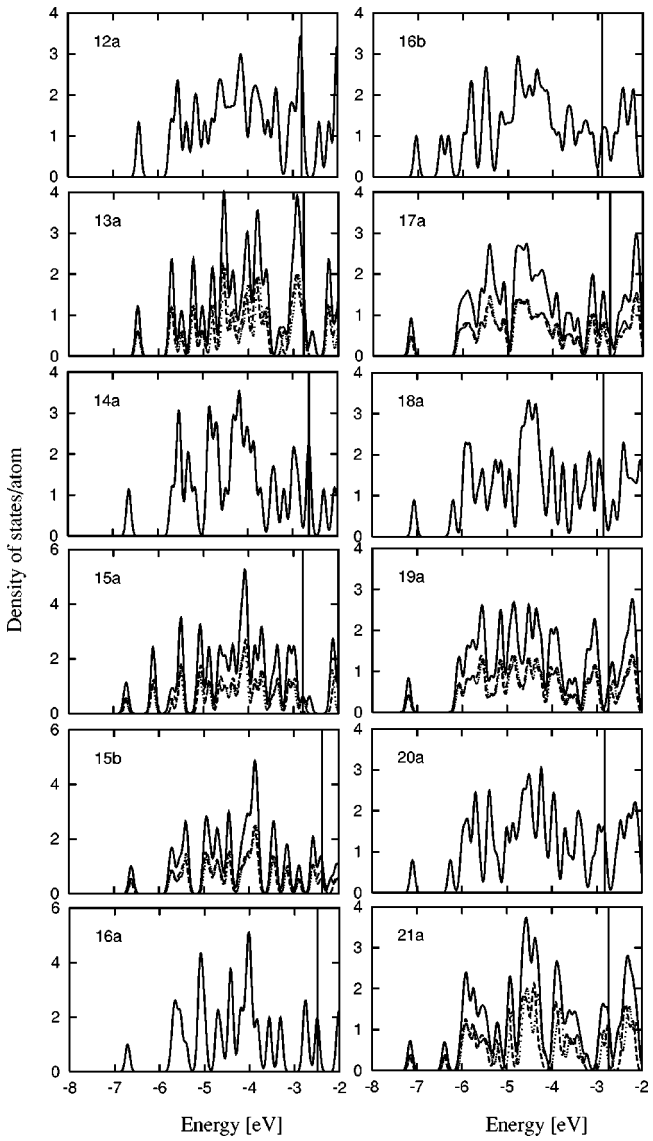

FIG. 7. Same as in Fig. 6. For $N=15$ and 16 we have given the spectra of both the cubic (15a and 16b) as well as the hexagonal (15b and 16a) isomers.

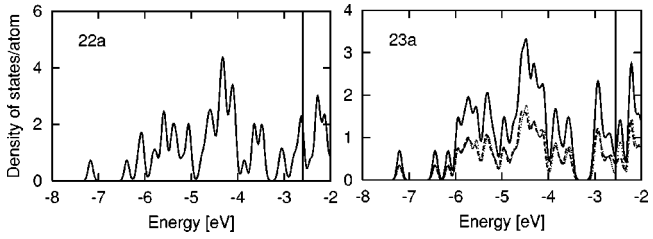

FIG. 8. Same as in Fig. 6 for $N=22$ and 23.

First, it is interesting to note that in the photoemission spectra[2] also there are two to three peaks with some fine structure in a range of about 1.25 eV. This is in general agreement with our results. However, the experimental band widths are narrower and suggest that correlation effects may be important for small clusters. The photoemission spectra of some clusters with even number of atoms show a peak at low binding energies that is separated from the main emission. This corresponds to the HOMO of the anion and is indicative of a large HOMO-LUMO gap in the corresponding neutral cluster. In particular, the photoemission spectra of 4-, 6-, 8-, and 10-atom clusters show the HOMO of Nb_4^- to be at the lowest binding energy. From calculations also we find the LUMO of Nb_4 to lie at lower binding energy than those for 6- and 8-atom clusters. However, for Nb_{10}, the calculated LUMO again lies at nearly the same energy as for Nb_4. The HOMO-LUMO gaps (Table I) for Nb_4 and Nb_{10} are the largest among all the clusters studied here. Another notable feature is that for small clusters with 3 or 4 atoms, more states are in the energy region of -3.5 eV but for larger clusters the peaks are more significant in the region of -4 to -5 eV. This agrees well with the observed behavior.

For Nb_9, two isomers lie very close in energy and both of these are likely to be present in experiments. We have shown the density of states for both the isomers in Fig. 6. For the second isomer (9b), there is a significant peak at around -5.5 eV which is also in agreement with significant emission in experiments in the high energy region. For $N>10$, the calculated spectra become broader and this is generally in agreement with experiments. However, photoemission data show sharper features for Nb_{15}^- as compared to those obtained for other clusters in this range. While a quantitative comparison of widths and heights is difficult, also due to the charged nature of clusters in the experiments, the calculated spectra for both the cubic and the hexagonal isomers of Nb_{15} have peaks in the high binding energy region and a strong peak at around -4.0 eV with broader features on either side. This is in good qualitative agreement with experiments. Another interesting comparison is for 17- and 19-atom clusters. The photoemission data show a weak peak at low binding energies near the HOMO in both the cases. It can be seen in Fig. 7 that for neutral Nb_{17} and Nb_{19} clusters, there are significant peaks near the HOMO followed by a region of low DOS and then a broad band around -5 eV. In experiments also this corresponds to the main peak for these clusters. For Nb_{21} and Nb_{22}, the DOS has a sharp feature in the middle of the band presumably due to the more symmetric nature of the cluster. The DOS of Nb_{23} is similar (Fig. 8) to the one for Nb_{22}.

An interesting result of the electronic structure is the variation in the HUMO-LUMO gap with size. This is shown in Fig. 9. The calculated gap is largest for $N=4$. However, experimental values are given in the range of 6- to 25-atom clusters and therefore, this can not be compared with experiments. It is noted that odd atom clusters have small gaps and there is an even-odd alternation in the gap behavior as also obtained experimentally.[2] Clusters with 8, 10, and 16 atoms have large gaps while those with 12 and 14 atoms, smaller.

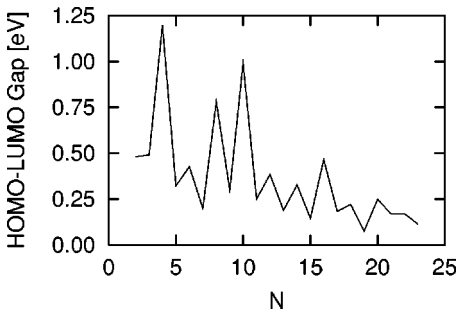

FIG. 9. HOMO-LUMO gap as a function of the cluster size.

This result agrees with experiments and also with the low reactivity of 8-, 10-, and 16-atom clusters. The calculated values are in good agreement with those obtained from experiments in the case of 8- and 16-atom clusters whereas for Nb_{10}, the calculated value of the gap is slightly higher than the one obtained from photoemission data. In experiments, there is a possibility of the presence of isomers which can affect the measurements. From Table I, it is seen that the isomer (10b) has significantly lower HOMO-LUMO gap though the BE is only slightly different from (10a). However, the large gap for Nb_{10} agrees with the finding that its reactivity is the lowest. In other cases the HOMO-LUMO gaps are small and these are again in good agreement with the experimental data. Of particular mention is the small gap for Nb_{15}. Therefore, it is not surprising that it is also reactive in spite of its bcc closed atomic shell structure.

C. Stability and magic behavior

Large gaps are good indicators of the stability of clusters. However, the BEs are also important and as our results show, niobium clusters are good examples. In Fig. 10, we have shown BE per atom and the second order difference of the total energy to obtain the magic behavior. The calculated BE's agree well with the available experimental data. Overall the calculated values seem to be slightly underestimated. However, the overall trend as well as the fragmentation energies (see later) are in very good agreement with experiments. The second order difference in energy shows 4-, 8-, 10-, 15-, and 16-atom clusters to be magic and these should be abundant. In addition, 7- and 12-atom clusters are weakly

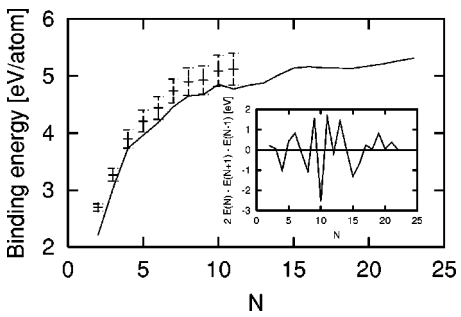

FIG. 10. Plot of the variation of the binding energy per atom as a function of the cluster size. The experimental points are shown by error bars. Also shown in the inset is the second order difference in energy. The negative values indicate magic behavior.

TABLE III. The BE (eV/atom), HOMO-LUMO gap (eV) and the nearest neighbor bond lengths (Å) for M_{10} clusters.

M	BE	Gap	*d*
V	3.17	0.92	2.12–2.57
Nb	4.85	0.99	2.43–2.86
Ta	5.99	0.83	2.51–2.76

magic while 3-, 14-, 18-, 20-, and 22-atom clusters are at the boundary. The magic behavior of 8-, 10-, and 16-atom clusters is in agreement with the HOMO-LUMO gap data. However, the stability of Nb_{15}, presumably due to atomic shell closing, is very intriguing and it endorses the fact that its reactivity should be due to the small HOMO-LUMO gap. There is a significant gap of about 0.6 eV above the LUMO and therefore, Nb_{15}^- is likely to be strongly abundant with electronic as well as atomic shell closing. The magic behavior of Nb_{15} is in contrast to the *sp* bonded metal clusters for which the magic clusters also have a large gap and in general clusters with odd number of electrons are not magic. A large HOMO-LUMO gap of 0.5 eV also exists above the LUMO of Nb_7 and therefore, Nb_7^- should also be strongly abundant. It is interesting to note that from the energetic point of view, *Nb_6 is not magic though its HOMO-LUMO gap is nearly equal to that of Nb_{16}*. Another important result is that *Nb_{13} is not magic*. However, Nb_{13}^- has a gap of 0.36 eV above HOMO and it can also be abundant. As the cluster size increases, the gaps become smaller and therefore, all clusters should be reactive as it is indeed also found experimentally for hydrogen.[3] In general, the magic behavior of niobium clusters is found to be different from those known[1] for other transition metals in the beginning and the end of a *d* series.

D. V_{10} and Ta_{10}

The particular stability of Nb_{10} and the existence of large HOMO-LUMO gap suggest that a similar behavior could arise for V_{10} and Ta_{10} clusters due to the band narrowing as V and Ta are isoelectronic and have the same bcc structure in bulk. To confirm this viewpoint, we studied the electronic structure of V_{10} and Ta_{10} clusters. For vanadium, we considered the 3*p* states also as valence, while for tantalum, the calculations were performed by considering only five valence electrons per Ta atom. The HOMO-LUMO gaps in all the three cases are comparable but it is the largest for Nb_{10}. The calculated BEs, gaps and structural data are given in Table III. The structures of these clusters are similar. An important aspect is the dimerization which is most prominent for V_{10}. It has the shortest bond length of 2.12 Å and the longest nearest neighbor bond, 2.57 Å. As one goes from V to Nb to Ta, the dimerization becomes weaker and for Ta_{10}, the nearest neighbor bond lengths vary in the range of 2.51–2.76 Å only. The DOSs for the 10-atom clusters of these elements are compared in Fig. 11. It shows an overall broadening of the *d* band in going from V_{10} to Ta_{10}. This is expected due to the broader extent of the 5*d* states. The features in the DOS of V_{10} and Nb_{10} (Fig. 6) are quite similar. However, for Ta_{10}, the peaks and the gaps are less prominent as the states are more spread.

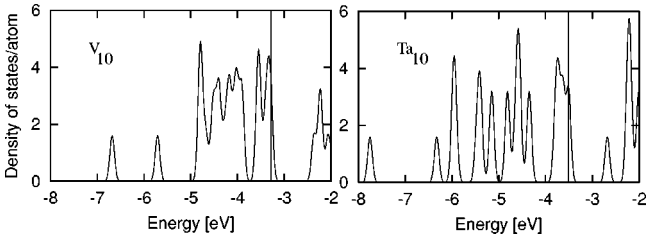

FIG. 11. Density of states plots for 10-atom clusters of V and Ta.

E. Fragmentation behavior

The fragmentation behavior of clusters is shown in Fig. 12. It is found that in most cases, dissociation of a monomer is energetically the most favorable channel. These results are in very good agreement with the experimental data (also shown in the figure) except for $N=2$ and 11 for which the calculated values are lower. This gives us confidence that the lowest energy structures obtained here are likely to be the ground states of niobium clusters. For a few clusters with $N>11$, fragmentation into two subclusters become either competitive or even the lowest energy channel. However, experimental results[23] are available only up to $N=11$. The energies for different clusters and low energy fragmentation channels are given in Table IV. It is seen that for Nb_4, (1,3) and (2,2) are competitive. This agrees also with experiments. For Nb_{12} and Nb_{14}, the lowest energy fragmentation channels are, respectively, (2,10) and (4,10). The latter corresponds to magic clusters. For $N=10$, 13, 18, and 20, the next lowest energy channels are (2,8), (3,10), (2,16), and (4,16), respectively. In all these cases, at least one cluster is magic. Further, for Nb_4, Nb_8, Nb_{10}, Nb_{14}, Nb_{15}, Nb_{22}, and Nb_{23}, the fragmentation energies are locally highest. These are also

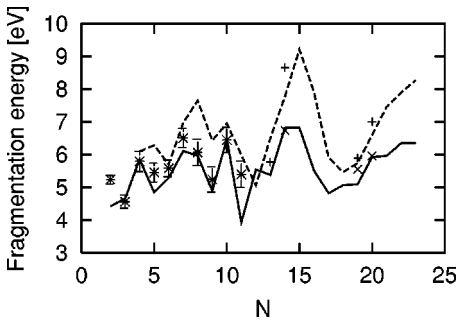

FIG. 12. Low fragmentation energy channels of niobium clusters. In most cases fragmentation of Nb_N into a Nb atom and Nb_{N-1} cluster is most favorable (full line). But for some clusters fragmentation into two subclusters is either competitive or is the lowest energy process. The dotted line shows fragmentation into a dimer and a Nb_{N-2} cluster. Plus and cross show fragmentation energies with one product to be Nb_3 and Nb_4, respectively. The calculated values are in excellent agreement with experimental data shown by error bars.

TABLE IV. The fragmentation energies, E_M in eV for an N atom cluster to fragment into Nb_M and Nb_{N-M} clusters. Expt. values are taken from Ref. 23.

N	E_1	E_2	E_3	E_4	Expt.
2	4.43				5.24 ± 0.13
3	4.67	4.67			4.57 ± 0.20
4	5.86	6.10	5.86		5.80 ± 0.31
5	4.85	6.29	6.29	4.84	5.46 ± 0.29
6	5.29	5.71	6.91	5.71	5.59 ± 0.25
7	6.12	6.98	7.16	7.16	6.51 ± 0.30
8	5.97	7.66	8.27	7.27	6.07 ± 0.40
9	4.90	6.44	7.89	7.31	5.25 ± 0.39
10	6.49	6.95	8.25	8.51	6.45 ± 0.39
11	3.94	6.00	6.22	6.33	5.40 ± 0.40
12	5.55	5.06	6.88	5.91	
13	5.39	6.51	5.78	6.40	
14	6.83	7.78	8.66	6.74	
15	6.82	9.22	9.94	9.62	
16	5.52	7.91	10.07	9.59	
17	4.83	5.92	8.07	9.03	
18	5.07	5.47	6.32	7.28	
19	5.10	5.75	5.90	5.56	
20	5.93	6.60	7.01	5.97	
21	5.97	7.47	7.90	7.11	
22	6.35	7.90	9.15	8.39	
23	6.36	8.28	9.58	9.65	

the magic clusters except for Nb_{23} in which case we have not done calculations on Nb_{24}. For Nb_{19}, many fragmentation channels are competitive (Table IV) and this may also be a reason for its low abundance. These results also show that the self-adsorption energies which are the opposite of the single atom fragmentation energies are the largest for clusters with $N=N_m-1$, where N_m corresponds to a magic cluster.

IV. SUMMARY

In summary, we have presented *ab initio* calculations of the growth behavior and the evolution of the electronic structure of niobium clusters. For small clusters the growth is based either on a tetrahedron or a prism, but for clusters with $N>13$, high coordination structures based on hexagonal layers become more favorable. In particular, icosahedral growth is not favored in niobium clusters. Nb_{15} is distinct and has a slightly distorted bcc structure. An interesting result is the tendency for dimerization in Nb_{10}. This tendency is even more prominent for the isoelectronic V_{10}, but it reduces for Ta_{10}. The lowest energy structures have lowest spin in all the cases except for Nb_2. The electronic structures of clusters show large HOMO-LUMO gaps for 4-, 6-, 8-, 10-, 12-, 14-, and 16-atom clusters. This agrees well with the low reactivity of 6-, 8-, 10-, 12-, and 16-atom clusters. However, Nb_6 is not magic. These results show different behavior of clusters with regard to their stability and reactivity. The calculated binding energies, fragmentation behavior, gaps, and the electronic structures are in good agreement with experimental data and provide support for the theoretical results of the structures presented here.

ACKNOWLEDGMENTS

V.K. thankfully acknowledges the kind hospitality at the Institute for Materials Research and the staff of the Center for Computational Materials Science at IMR-Tohoku University for making the Hitachi SR2201, SR8000, Compaq GS320 and the HITAC S-3800 supercomputers available and for their cooperation.

[1] V. Kumar, K. Esfarjani, and Y. Kawazoe, in *Clusters and Nanomaterials*, Springer Series in Cluster Physics (Springer Verlag, Heidelberg, 2001), p. 9.
[2] H. Kietzmann, J. Morenzin, P.S. Bechthold, G. Ganteför, and W. Eberhardt, J. Chem. Phys. **109**, 2275 (1998).
[3] M.E. Geusic, M.D. Morse, and R.E. Smalley, J. Chem. Phys. **82**, 590 (1985).
[4] A. Berces, P.A. Hackett, L. Lian, S.A. Mitchell, and D.M. Rayner, J. Chem. Phys. **108**, 5476 (1998).
[5] E.K. Parks, B.J. Winter, T.D. Klots, and S.J. Riley, J. Chem. Phys. **94**, 1882 (1991); T.D. Klots, B.J. Winter, E.K. Parks, and S.J. Riley, *ibid.* **95**, 8919 (1991).
[6] L. Holmgren, M. Andersson, and A. Rosen, Surf. Sci. **331-333**, 231 (1995).
[7] R.L. Whetten, M.R. Zakin, D.M. Cox, D.J. Trevor, and A. Kaldor, J. Chem. Phys. **85**, 1697 (1986).
[8] D.G. Pettifor, J. Phys. C **3**, 366 (1970).
[9] M. Sakurai, K. Watanabe, K. Sumiyama, and K. Suzuki, J. Chem. Phys. **111**, 235 (1999).
[10] Y. Tai (private communication).
[11] C. Berg, M. Beyer, U. Achatz, A. Joos, G. Niedner-Schatteburg, and V.E. Bondybey, J. Chem. Phys. **108**, 5398 (1998).
[12] M.R. Zakin, R.O. Brickman, D.M. Cox, and A. Kaldor, J. Chem. Phys. **88**, 3555 (1988).
[13] L. Goodwin and S.R. Salahub, Phys. Rev. A **47**, R774 (1993).
[14] H. Kietzmann, J. Morenzin, P.S. Bechthold, G. Ganteför, and W. Eberhardt, Phys. Rev. Lett. **77**, 4528 (1996).
[15] R. Fournier, T. Pang, and C. Chen, Phys. Rev. A **57**, 3683 (1998).
[16] H. Grönbeck and A. Rosen, Phys. Rev. B **54**, 1549 (1996).
[17] H. Grönbeck, A. Rosen, and W. Andreoni, Phys. Rev. A **58**, 4630 (1998).
[18] A.D. Becke, Phys. Rev. A **38**, 3098 (1988).
[19] C.L. Lee, W. Yang, and R.G. Parr, Phys. Rev. B **37**, 785 (1988).
[20] Vienna *ab initio* simulation package, Technische Universität Wien, 1999; G. Kresse and J. Furthmüller, Phys. Rev. B **55**, 11 169 (1996); Comput. Mater. Sci. **6**, 15 (1996).
[21] D. Vanderbilt, Phys. Rev. B **41**, 7892 (1990).
[22] J. P. Perdew, in *Electronic Structure of Solids' 91*, edited by P. Ziesche and H. Eschrig (Akademie Verlag, Berlin, 1991).

[23] D.A. Hales, L. Lian, and P.B. Armentrout, Int. J. Mass Spectrom. Ion Processes **102**, 269 (1990).
[24] M.D. Morse, Chem. Rev. **86**, 1049 (1986).
[25] V. Kumar and Y. Kawazoe, Phys. Rev. B **63**, 075410 (2001); V. Kumar and Y. Kawazoe, Scr. Mater. **44**, 1949 (2001).
[26] H. Cheng and L.-S. Wang, Phys. Rev. Lett. **77**, 51 (1996); L.-S. Wang, H. Wu, and H. Cheng, Phys. Rev. B **55**, 12 884 (1997).